Robotica (2012) volume 30, pp. 1167–1175. © Cambridge University Press 2012
doi:10.1017/S0263574711001287

Modeling and assessment of the backlash error of an industrial robot

Mohamed Slamani, Albert Nubiola and Ilian A. Bonev*

École de Technologie Supérieure, Montreal, QC, Canada

(Accepted November 28, 2011. First published online: January 16, 2012)

SUMMARY

This paper proposes an experimental approach for evaluating the backlash error of an ABB IRB 1600 industrial serial robot under various conditions using a laser interferometer measurement instrument. The effects of the backlash error are assessed by experiments conducted on horizontal and vertical paths. A polynomial model was used to represent the relationship between the backlash error and the robot configuration. A strategy based on statistical tests was developed to choose the degree of polynomial representing the effect of the tool center point (TCP) speed and payload. Results show that the backlash error strongly affects the repeatability of the industrial robot. Statistical analyses prove that the backlash is highly dependent on both robot configuration and TCP speed, whereas it remains nearly unaffected by changes in the payload. It was discovered that the backlash error as measured at the TCP may exceeds 100 μm, and that the positive backlash error increases and the negative backlash error decreases when there is increase in TCP speed.

KEYWORDS: Serial industrial robot; Backlash; Repeatability; Laser interferometer; Statistical tests.

1. Introduction

Industrial robots have become an indispensable means of automation to increase productivity and flexibility of production systems. Consequently, the characterization and improvement of the robot performance in terms of accuracy have become increasingly important in modern manufacturing and especially in the aerospace sector.[1]

These days, two measures are commonly used for describing the positioning performance of industrial robots – *repeatability* and *accuracy* – and ISO 9283:1998[2] is the international norm specifying how these and many other performance criteria should be evaluated.

The accuracy of an industrial robot is primarily affected by the geometric errors caused by mechanical–geometrical imperfections such as link parameter errors, flexibility and wear of the robot structure elements, the non-uniform thermal expansion of the robot structure, backlash (hysteresis), encoder resolution errors, coordinate transformation errors, and control errors.[3] In the case of *bidirectional* accuracy and repeatability, the backlash is one of the most important factors affecting the performance of industrial robots.[4] Bidirectional repeatability is important whenever a robot is sent to both manually taught configurations and configurations that are calculated online (e.g., using a camera or a touch probe). It is frequently the most serious problem associated with geared transmissions. Although required for proper tooth action, too much backlash may lead to unacceptable robot repeatability. Accordingly, the backlash effects should be checked frequently and techniques for measuring and identifying it are required.

The effects of backlash in robotic systems can be reduced by either using identification techniques,[5–8] control techniques,[9,10] compensation techniques,[11] or by using precision gears (e.g., as in most Stäubli industrial robots). However, the last solution raises the manufacturing cost of industrial robots and is practically insufficient to eliminate the backlash effect because there are several sources of the effect that are impossible to remove completely.[5]

Ruderman *et al.*[12] present an approach to the modeling and identification of elastic robot joints with hysteresis and backlash. The distributed model parameters are identified from the experimental data obtained from internal system signals and external angular encoder mounted to the second joint of a 6-degree of freedom (DOF) industrial robot.

Assessing the bidirectional positioning performance of an industrial robot is a very complex task that requires expensive metrology equipment. In 1995, the International Standards Organization (ISO) published a guide[13] (ISO TR 13309) on test equipment and metrology methods for robot performance evaluation in accordance with ISO 9283.[3] However, the bidirectional positioning performance is not described in this ISO guide and is never mentioned in the technical specifications of an industrial robot. Furthermore, various tests can be performed with low-cost tooling such as digital indicators (comparators) and reference objects, but the most common equipment used for robot calibration and accuracy assessment remains the laser tracker. Indeed, a laser tracker is relatively simple to use and can quasi-continuously (typically every millisecond) measure the position of a single spherically mounted reflector (SMR) or even measure the complete pose in static mode (by measuring the positions of three SMRs, however, using the so-called ADM mode, which is less accurate) in the entire workspace of an industrial robot. Unfortunately, laser trackers are excessively expensive ($100K and more) and very sensitive to air turbulences. Furthermore, their volumetric accuracy and repeatability are much worse than those of a high-precision, single-axis

* Corresponding author. E-mail: ilian.bonev@etsmtl.ca

measurement instrument commonly used for machine tool calibration such as the laser interferometer system. Yet, with the exception of a few papers,[4,14] this instrument is rarely used in conjunction with industrial robots.

In the field of machine tools, Slamani *et al.*[15] developed a strategy based on statistical tests to choose the degree and then select the most useful terms for a representative polynomial for each joint motion error with the integration of terms for motion hysteresis (backlash). This method is applied to direct experimental calibration data of all of the joint motion errors along the maximum stroke allowable by the machine tool axes using laser interferometry.

In this paper, we use a statistical method to evaluate in an optimal way the relationship between backlash, robot configuration, TCP speed, and payload based on experimental tests conducted on a non-calibrated ABB IRB 1600 industrial (serial) robot using the Renishaw laser interferometer system. Furthermore, some important characteristics of the backlash error are identified.

2. Representation Model for Backlash

2.1. Definition of backlash

It is known that backlash occurs when the direction of motion of an actuated joint is reversed. In this paper, limited by the nature of our measurement instrument, we focus on the backlash along a linear path rather than the backlash in each revolute joint. Indeed, the backlash along a linear path occurs when the robot end-effector changes its direction of motion.

Let x_i, τ_i be the data associated with the measurement of a robot's one-dimensional position error, with τ_i being the experimental value of the position error (difference between measured and nominal position) at a particular nominal coordinate x_i, i.e., at pose i, along the linear path, where $i = 1, 2, \ldots, n$. To evaluate the effect of the backlash error along the linear path, the tests have to be bidirectional. Each test run is repeated m times, which means that there are multiple observations of τ_i for the same nominal value of x_i. The total number of measurements are $n_t = nm$, for each direction. The backlash error along the linear path can be defined as the difference between the position errors for forward and backward direction motions with respect to the target pose:

$$y_i = \tau_i^{\uparrow} - \tau_i^{\downarrow}, \tag{1}$$

where y_i is the backlash error for pose i, and $\tau_i^{\uparrow}$ and $\tau_i^{\downarrow}$ are the position errors for pose i for the forward and backward directions, respectively.

According to Eq. (1), the backlash error is null if the position errors in the forward ($\tau_i^{\uparrow}$) and backward ($\tau_i^{\downarrow}$) directions are identical. On the other hand, a positive backlash occurs if the position error in the forward direction is bigger than the position error in the backward direction.

2.2. Relationship between backlash and robot configuration

The first objective is to find the sufficient polynomial of degree p (with $p < n$), which adequately represents the systematic contents of a backlash. The polynomials are of the form

$$\bar{y}_i = \beta_0 + \beta_1 x_i + \beta_2 x_i^2 + \cdots + \beta_p x_i^p + \varepsilon_i, \tag{2}$$

where ε_i is the random error in backlash for pose i, and $\bar{y}_i$ is the mean backlash at pose i (recall that we take $2m$ measurements at each pose). This linear system of n equations with $p + 1$ unknowns as the coefficients of the polynomial can be estimated using the least squares method. However, the choice of degree and terms of the polynomial is a more delicate and critical task as it conditions the polynomial's representativity.

In order to achieve this, a statistical technique is applied successively based on the lack-of-fit test. Equation (2) can be written as

$$\begin{bmatrix} \bar{y}_1 \\ \bar{y}_2 \\ \vdots \\ \bar{y}_n \end{bmatrix} = \begin{bmatrix} 1 & x_1 & x_1^2 & \cdots & x_1^p \\ 1 & x_2 & x_2^2 & \cdots & x_2^P \\ \vdots & \vdots & \vdots & & \vdots \\ 1 & x_n & x_n^2 & \cdots & x_n^p \end{bmatrix} \begin{bmatrix} \beta_0 \\ \beta_1 \\ \vdots \\ \beta_p \end{bmatrix}, \tag{3}$$

or in matrix form as

$$\bar{\mathbf{y}} = \mathbf{X}\mathbf{p}. \tag{4}$$

Since matrix $\mathbf{X}$ is in general rectangular, a solution is found by

$$\mathbf{p} = \mathbf{X}^{+}\bar{\mathbf{y}}, \tag{5}$$

where $\mathbf{X}^{+}$ is the Moore–Penrose pseudo inverse of the observation matrix $\mathbf{X}$ (Vandermonde matrix), $\mathbf{p}$ is the vector of coefficients, and $\bar{\mathbf{y}}$ is the vector of means of backlash measurements.

Now, let us first represent the average of the observations (backlash) for various values of coordinates x_i by a polynomial of the first order:

$$\bar{y}_i = \beta_0 + \beta_1 x_i + \varepsilon_i. \tag{6}$$

If this model is not adequate, we then add other terms to the equation.

The higher degree terms $x^j (j > 1)$ are introduced one by one, but before introducing a term of degree $(j + 1)$, a test on the lack-of-fit makes it possible to check whether the improvement made by the jth degree term is significant. The lack-of-fit test consists in calculating the variance ratio, or F-ratio, between the mean squares for the lack-of-fit test, denoted as *MSLF*, and the mean squares pure error, denoted as *MSPE*:

$$F = \frac{MSLF}{MSPE}, \tag{7}$$

where

$$MSLF = \frac{SSLF}{n - p - 1}, \tag{8}$$

$$MSPE = \frac{SSPE}{n_t - n}, \tag{9}$$

https://doi.org/10.1017/S0263574711001287 Published online by Cambridge University Press

Table I. Summary of the lack-of-fit test.

Source	Sum	DOFs	Mean	F-ratio	Degree of polynomial
Lack-of-fit	*SSLF*	$n-p-1$	*MSLF*	F	p
Pure error	*SSPE*	n_t-n	*MSPE*		
Residual	*SSE*	n_t-p-1			

and *SSLF* is the lack-of-fit sum of squares, while *SSPE* is the pure error sum of squares. We will assume that *SSLF* is due to an inappropriate choice of model such as the degree of the polynomial. *SSLF* is the difference in the sum of squares error (*SSE*) of the proposed model and the inherent data dispersion about the mean, i.e., the pure error sum of squares (*SSPE*). The pure error measures the random fluctuations or inherent scatter in the response variable at each position. The pure error is calculated as follows and does not depend on any particular model,[16]

$$SSPE = \sum_{i=1}^{n}\sum_{u=1}^{m}(y_{i,u} - \bar{y}_i)^2, \tag{10}$$

where $y_{i,u}$ is the backlash errors for pose i and repetition u.

Once a model has been proposed, we can calculate *SSE* as

$$SSE = \sum_{i=1}^{n}\sum_{u=1}^{m}(y_{i,u} - \hat{y}_i)^2, \tag{11}$$

where $\hat{y}_i$ is the estimate model for the backlash error. Then *SSLF* is obtained as follows:

$$SSLF = SSE - SSPE, \tag{12}$$

where *SSPE* is the pure error sum of squares and has $n_t - n$ DOFs, *SSE* is the unexplained variation or the sum of square errors and has $n_t - p - 1$ DOFs, and *SSLF* is the lack-of-fit sum of squares and has $n - p - 1$ DOFs.

The null and alternative hypotheses for testing for the lack-of-fit would be

H_0: there is no lack-of-fit in the regression model;
H_1: there is a lack-of-fit in the regression model.

The usual procedure is then to compare the $F = \frac{MSLF}{MSPE}$ ratio with $F_{\alpha;n-p-1;n_t-n}$, which is the critical value given by the Fisher's table at threshold $\propto = 0.05$. This statistical test makes it possible to test the following hypotheses:

$$H_0 : E(y) = \beta_0 + \beta_1 x, \tag{13}$$

$$H_1 : E(y) \neq \beta_0 + \beta_1 x. \tag{14}$$

The decision criteria is to reject H_0 if $F > F_{\alpha;n-p-1;n_t-n}$, if not, then the hypothesis according to which the linear model is adequate is confirmed.

If H_0 is rejected, then we add another coefficient to the model and repeat the same test but for the new polynomial until the hypothesis of adjustment of the model is confirmed. A summary of the lack-of-fit test is presented in the format of Table I.

2.3. Relationship between backlash and TCP speed, and between backlash and payload

The model described so far comprises only quantitative variables (positions) and only for one state. Since the backlash may change as a function of state (change in TCP speed or payload), the presence or absence of each state enables us to integrate it in the model by an auxiliary variable of qualitative nature (indicator variable). The auxiliary variable takes values of 0 or 1.

Let us suppose that after the lack-of-fit test our model for the backlash at state 1 has the following form:

$$\bar{y}_i = \beta_0 + \beta_1 x_i + \beta_2 x_i^2 + \varepsilon_i. \tag{15}$$

Let us add the qualitative variable (effect of the TCP speed or payload) using an auxiliary variable (indicator variable) D, where

$D = 0$ if the robot is in state 1 (position only);
$D = 1$ if the robot is in state 2 (presence of position and the TCP speed or position and payload).

The regression model is then

$$\bar{y}_i = \beta_0 + \beta_1 x_i + \beta_2 x_i^2 + \beta_0' D + \varepsilon_i. \tag{16}$$

This system can be written in matrix form as follows:

$$\begin{bmatrix} \bar{y}_1^{st_1} \\ \bar{y}_2^{st_1} \\ \vdots \\ \bar{y}_n^{st_1} \\ \bar{y}_1^{st_2} \\ \bar{y}_2^{st_2} \\ \vdots \\ \bar{y}_n^{st_2} \end{bmatrix} = \begin{bmatrix} 1 & x_1 & x_1^2 & 0 \\ 1 & x_2 & x_2^2 & 0 \\ \vdots & \vdots & \vdots & \vdots \\ 1 & x_n & x_n^2 & 0 \\ 1 & x_1 & x_1^2 & 1 \\ 1 & x_2 & x_2^2 & 1 \\ \vdots & \vdots & \vdots & \vdots \\ 1 & x_n & x_n^2 & 1 \end{bmatrix} \begin{bmatrix} \beta_0 \\ \beta_1 \\ \beta_2 \\ \beta_0' \end{bmatrix}, \tag{17}$$

where $\bar{y}_i^{st_1}$ and $\bar{y}_i^{st_2}$ are the averages of the observations of the backlash error for state 1 and state 2, respectively.

The solution of the linear system (17) provides the least squares estimation of the coefficients of the model. The statistical tests for the marginal contribution of the auxiliary variable are typically based on the Student's t distribution:[16]

$$t = \frac{b_j}{s(b_j)}, \tag{18}$$

where b_j are the coefficients and $s(b_j)$ are the standard errors of the regression coefficients b_j $(j = 0, 1, \ldots, p)$. The Student's test consists in testing the following hypothesis:

$$H_0 : \beta_0' = 0,$$
$$H_1 : \beta_0' \neq 0.$$

The decision criterion is to reject H_0 if $t > t_{\alpha/2;n-p-1}$ or $t < -t_{\alpha/2;n-p-1}$, if not, then the influence of the TCP speed or the payload prove to be insignificant (we favor the

https://doi.org/10.1017/S0263574711001287 Published online by Cambridge University Press

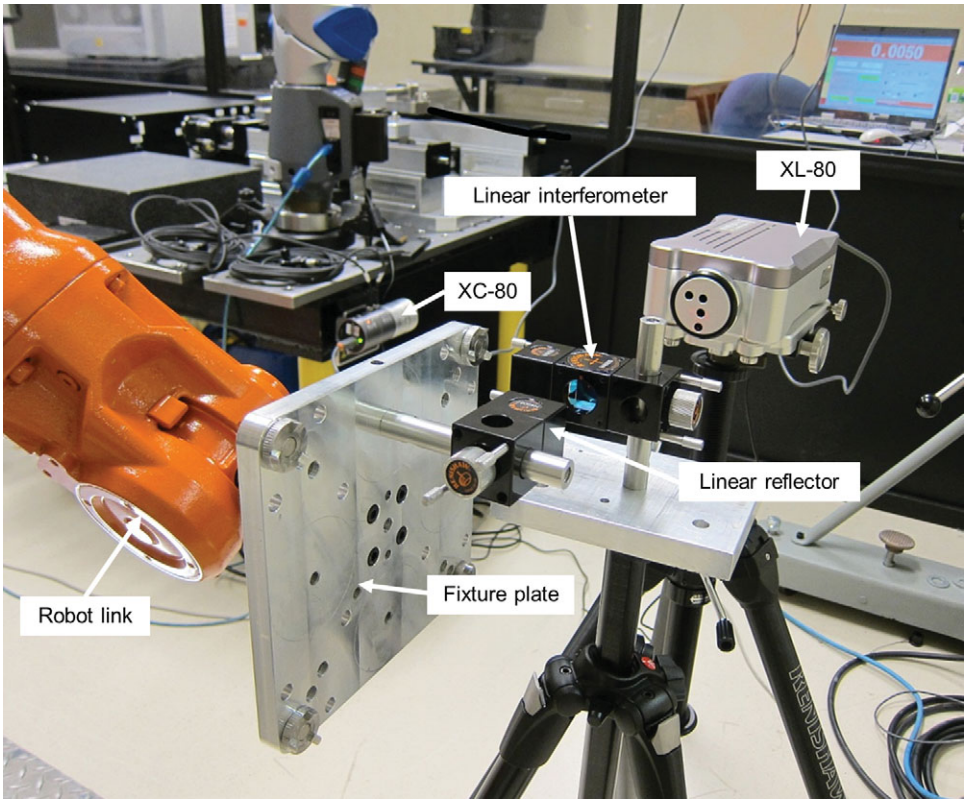

Fig. 1. (Colour online) Laser interferometer setup for measuring linear position errors along a linear path parallel to the y-axis of the base frame of the IRB1600 robot (the robot is at pose P_0).

hypothesis $H_0 : \beta'_0 = 0$), and consequently the two curves are superposed. The value of $t_{\alpha/2;n-p-1}$ is given by the Student's table. The model is then reduced to

$$\bar{y}_i = \beta_0 + \beta_1 x_i + \beta_2 x_i^2 + \varepsilon_i. \tag{19}$$

In contrast, if H_0 is rejected, we favor the hypothesis H_1, which means $\beta'_0 \neq 0$, indicating that the marginal contribution of the auxiliary variable D is significant at $\propto = 0.05$. The following step is to add, to the regression equation, other terms also sensitive to the qualitative variable (TCP speed or payload) but of higher degrees. The multiple regression models become

$$\bar{y}_i = \beta_0 + \beta_1 x_i + \beta_2 x_i^2 + \beta'_0 D + \beta'_1 D x_i + \varepsilon_i. \tag{20}$$

Considering all measurements available for states 1 and 2, Eq. (20) is written in matrix form as follows:

$$\begin{bmatrix} \bar{y}_1^{st_1} \\ \bar{y}_2^{st_1} \\ \vdots \\ \bar{y}_n^{st_1} \\ \bar{y}_1^{st_2} \\ \bar{y}_2^{st_2} \\ \vdots \\ \bar{y}_n^{st_2} \end{bmatrix} = \begin{bmatrix} 1 & x_1 & x_1^2 & 0 & 0 \\ 1 & x_2 & x_2^2 & 0 & 0 \\ \vdots & \vdots & \vdots & \vdots & \vdots \\ 1 & x_n & x_n^2 & 0 & 0 \\ 1 & x_1 & x_1^2 & 1 & x_1 \\ 1 & x_2 & x_2^2 & 1 & x_2 \\ \vdots & \vdots & \vdots & \vdots & \vdots \\ 1 & x_n & x_n^2 & 1 & x_n \end{bmatrix} \begin{bmatrix} \beta_0 \\ \beta_1 \\ \beta_2 \\ \beta'_0 \\ \beta'_1 \end{bmatrix}. \tag{21}$$

By the same method, the marginal contribution of the new term is tested:

$$\begin{aligned} H_0 &: \ \beta'_1 = 0, \\ H_1 &: \ \beta'_1 \neq 0. \end{aligned}$$

If H_0 is not rejected, the marginal contribution of the new term is insignificant at the threshold $\propto = 0.05$, and we conclude that the qualitative variable influence is significant and have a constant value equal to β'_0. The model becomes

$$\bar{y}_i = \beta_0 + \beta_1 x_i + \beta_2 x_i^2 + \beta'_0 D + \varepsilon_i. \tag{22}$$

In contrast, if H_0 is rejected, we favor H_1, which means that $\beta'_1 \neq 0$, hence we add another term in the model and follow the same procedure until we are able to fully represent the behavior of the qualitative variable.

3. Experimental Procedures

Tests were performed on an ABB IRB 1600–6/1.45 industrial robot installed in a laboratory facility with an ambient temperature in the range 22.4–23.3°C during the experiments. The robot was manufactured in 2008 and has never been in a collision accident. It neither has the *absolute accuracy* option (i.e., it is not calibrated) nor the *advanced shape tuning* option (for compensating the effects of friction at low speeds). A multi-purpose end-effector (well visible in Fig. 1) was used to mount the optics of the laser interferometer system. The weight of the end-effector in the linear position error setup is 2.23 kg. Steel discs can also be attached to the end-effector to increase its weight.

https://doi.org/10.1017/S0263574711001287 Published online by Cambridge University Press

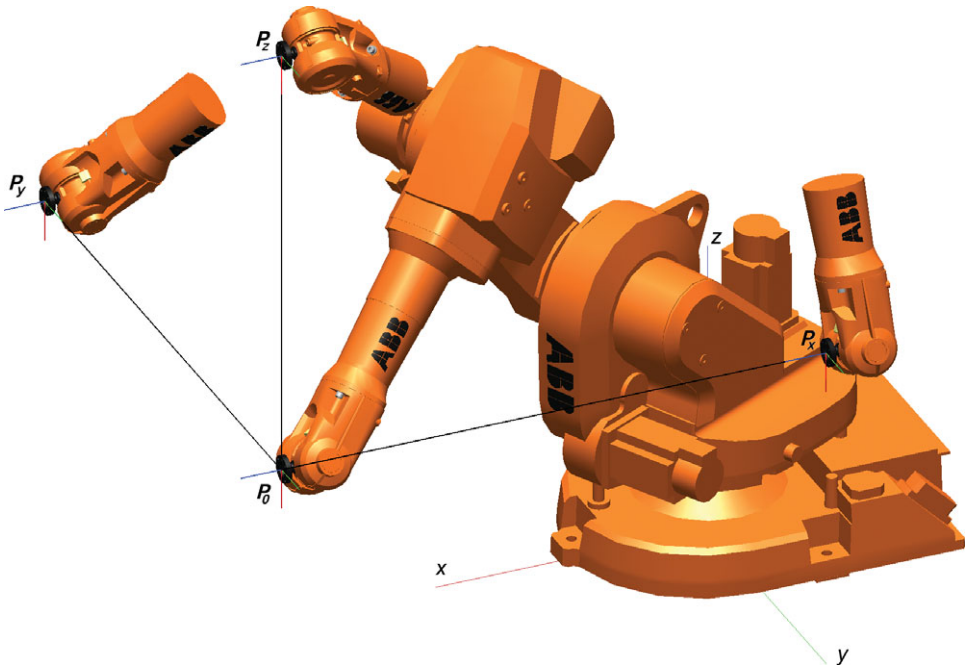

Fig. 2. (Colour online) Schematic showing the linear paths analyzed with the laser interferometer.

The measurement instrument used in this study is the latest model of Renishaw's laser interferometer system. The system is composed of an XL-80 laser unit, a XC-80 environmental compensation unit with external sensors, and measurement optics. The XL-80 laser unit and relevant optics installed in a setup for measuring linear position errors along a horizontal linear path is shown in Fig. 1. The XC-80 compensation system (attached to the steel table as shown in Fig. 1) very accurately measures air temperature, air pressure, and relative humidity, and accordingly compensates the wavelength of the laser beam. As a result, within a range of 1 m, the laser interferometer system has an accuracy of ± 0.5 μm and a resolution of 1 nm.

The XL-80 laser unit, in combination with different optic kits arranged in different setups, allows static measurements of five motion errors along a linear path – a *linear positional error* (along the linear path), two *straightness errors*, and two *angular errors* (about two orthogonal axes normal to the linear path).

The approximate locations of the centers of the linear measurement optics with respect to the robot flange frame (referred to by ABB as *tool0*) are $\{-65$ mm, 30 mm, 150 mm$\}$, for horizontal paths, and $\{-50$ mm, 0 mm, 150 mm$\}$ for vertical paths.

The robot was programmed to move along orthogonal linear paths, parallel to the axes of the robot base frame as shown in Fig. 2. The end-effector is kept at the same constant orientation for all linear paths (a 90° rotation about the base y-axis produces the orientation of the end-effector frame). The position component of pose P_0 is $\{1000$ mm, 500 mm, 600 mm$\}$ with respect to the robot base frame. The horizontal path is of length 1000 mm, while the vertical path is only 800-mm long. Each of the paths is divided uniformly into four segments and three new intermediate poses are calculated. For each of the two paths, the robot is programmed to move in linear bidirectional mode by starting 10 mm prior to pose P_0 (and along the linear path) and stopping at P_0, then at each of the three intermediate poses, and finally at the end of the path (i.e., at P_x, P_y, or P_z). At the end of the path, the robot program reverses the direction of travel and stops the end-effector at the same nominal points of measurement. A 10-mm overrun distance ensures that the first and last targets of a run are taken in the correct direction. The positive (forward) and negative (backward) motion directions allow the evaluation of the backlash error for each path. The sequence is repeated 10 times, and a pause of 5 s to allow full stabilization is done at each of the five measurement poses before a measurement is taken.

In order to assess the evolution of the backlash error as a function of the TCP speed and payload, the test is repeated four times at TCP speeds of 10, 1000, and 6000 mm/s and at payloads of 2.23 and 6 kg.

It is known that in laser interferometer tests, a dead-path error occurs when there is a significant separation between the optics at the datum position (i.e., P_0). To minimize the potential dead-path errors associated with datuming, the optics were positioned close together within 20 mm of one another when the laser is datumed (Fig. 1).

Finally, for each test, a warm-up sequence consisting of the actual motion error test trajectory was repeated during 1 h (from cold start), immediately followed by the actual test.

4. Results and Discussion

In accordance to ISO 9283:1998,[2] in this paper unidirectional r*epeatability* is defined as

$$RP_i = \pm 3\sigma_i = \pm 3\sqrt{\frac{\sum_{u=1}^{m}(\tau_{i,u} - \bar{\tau}_i)^2}{m-1}}, \qquad (23)$$

https://doi.org/10.1017/S0263574711001287 Published online by Cambridge University Press

where $\bar{\tau}_i$ is the arithmetic mean of the m repetitions at pose i.

Unidirectional repeatability refers to the repeatability at a pose when the arrival at that pose is from the same direction. It does not take into account the effects of backlash. Good bidirectional repeatability is typically more difficult to achieve than unidirectional repeatability because industrial robots have to deal with the backlash. Despite its importance, the bidirectional repeatability is never specified by the manufacturers of industrial robots, nor is described in the ISO 9283:1998[2] guide and is rarely the subject of performance assessments.

The backlash is defined as a component of bidirectional repeatability. The bidirectional repeatability is evaluated according to ISO 230–2[17] for machine tools as

$$R_i = \max\left(3\sigma_i^{\uparrow} + 3\sigma_i^{\downarrow} + |\bar{y}_i|, 6\sigma_i^{\uparrow}, 6\sigma_i^{\downarrow}\right), \qquad (24)$$

where $\bar{y}_i$ is the mean of the m measurements of the backlash for pose i defined as

$$\bar{y}_i = \bar{\tau}_i^{\uparrow} - \bar{\tau}_i^{\downarrow}, \qquad (25)$$

and $\bar{\tau}_i^{\uparrow}$ and $\bar{\tau}_i^{\downarrow}$ are the mean position errors for pose i for the forward and backward directions, respectively.

The readings of each linear position error are analyzed and tested statistically. Starting with the vertical axis, Fig. 3 shows the linear position errors along the path parallel to the base z-axis. The first observation is that the position unidirectional repeatability for forward and backward directions (i.e., $3\sigma_i^{\uparrow}$ and $3\sigma_i^{\downarrow}$) at each of the five poses along the linear path is independent of the TCP speed and payload. It is ranging between 8 μm and 23 μm. In contrast, results show that the bidirectional repeatability (i.e., R_i) is strongly affected by variation in the TCP speed and payload. The bidirectional repeatability for each case is in the following ranges: 36–80 μm for a payload of 2.23 kg and at a TCP speed of 10 mm/s, 75–134 μm for a payload of 2.23 kg and at a TCP speed of 6000 mm/s, and 43–75 μm for a payload of 6 kg and at a TCP speed of 10 mm/s.

Figure 4 shows the linear position errors along the path parallel to the base y-axis. Results show that the bidirectional repeatability and especially the unidirectional repeatability along the y-axis are much better than those along the z-axis.

For the tests with a payload of 2.23 kg and at a TCP speed of 10 mm/s, the lack-of-fit tests, summarized in Table II, show that the second-order model is sufficient to represent relationship between backlash error and robot configuration for the path parallel to the base z-axis because the ratio $F = 1.25$ is less than $F_{0.05,1,45} = 4.05$ from the Fisher's table. A second-degree polynomial was found sufficient to represent the backlash error for the path parallel to the base y-axis and the F-ratio is 0.0174.

Furthermore, the results of the Student's test illustrated in Fig. 5 show that the TCP speed has a significant contribution on the backlash and can be modeled as an offset since the test on the first coefficient β_0' gives $t = 3.49 > 2.45$, so hypothesis H_0 can be excluded. Furthermore, the test on the last coefficient β_1' gives $t = -0.7724 < 2.57$. Thus, hypothesis H_0 is not rejected, and the contribution of the

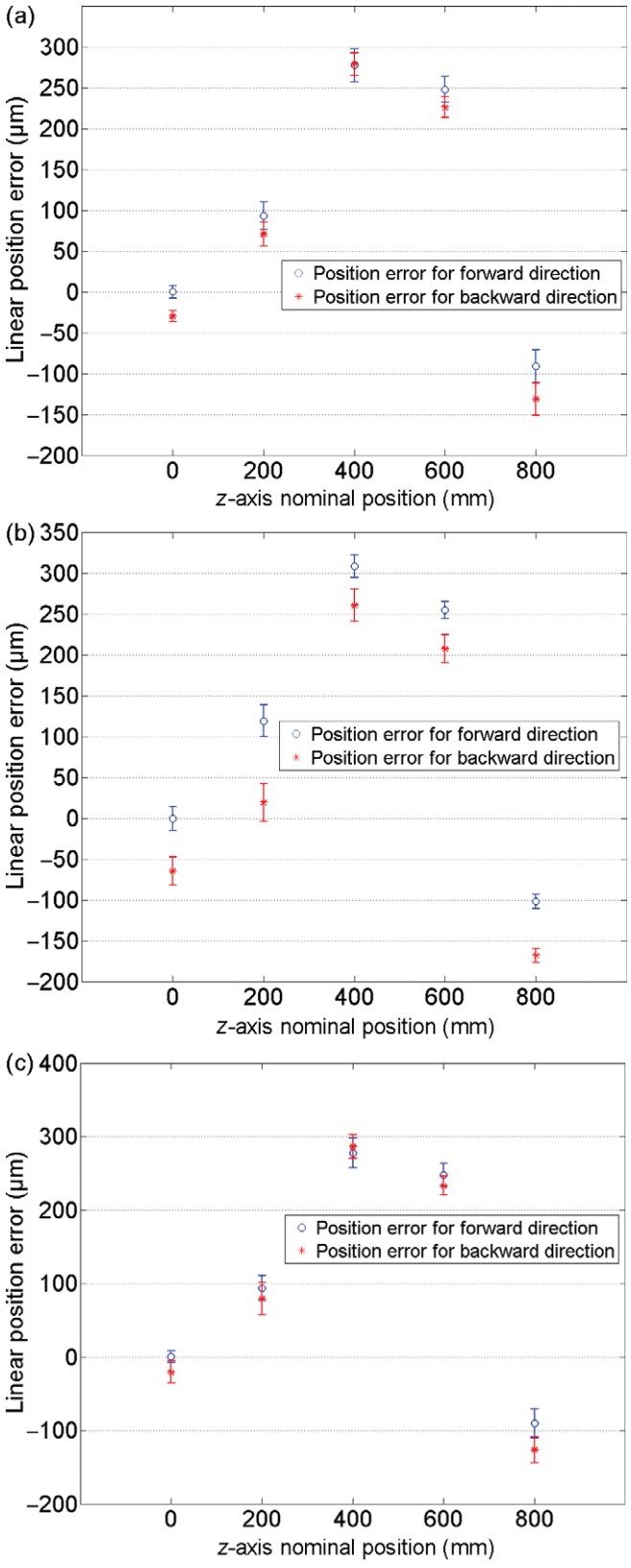

Fig. 3. (Colour online) Linear bidirectional position errors at five poses along the path parallel to the base z-axis. (a) Payload of 2.23 kg, TCP speed of 10 mm/s, $3\sigma_i^{\uparrow}$, $3\sigma_i^{\downarrow}$, and R_i are between 8 μm and 21 μm, 6 μm and 20 μm, and 36 μm and 80 μm, respectively; (b) payload of 2.23 kg, TCP speed of 6000 mm/s, $3\sigma_i^{\uparrow}$, $3\sigma_i^{\downarrow}$, and R_i are between 9 μm and 19 μm, 8 μm and 23 μm, and 75 μm and 134 μm, respectively; (c) payload of 6 kg, TCP speed of 10 mm/s, $3\sigma_i^{\uparrow}$, $3\sigma_i^{\downarrow}$, and R_i are between 8 μm and 21 μm, 12 μm and 20 μm, and 43 μm and 75 μm, respectively.

https://doi.org/10.1017/S0263574711001287 Published online by Cambridge University Press

Table II. Results of the lack-of-fit test for the backlash error with payload of 2.23 kg and at a TCP speed of 10 mm/s along the path parallel to the base z-axis.

Source	Sum	DOFs	Mean	F-ratio	p
Lack-of-fit	-4.21×10^{-4}	1	-2.1×10^{-4}	1.25	3
Pure error	76×10^{-4}	45	1.68×10^{-4}		
Residual	72×10^{-4}	46			

coefficient β_1' of the TCP speed is deemed insignificant at the threshold $\propto = 0.05$. Therefore, the estimated model is

$$\hat{y}_i = 33.83 - 0.0914x_i + 0.0001x_i^2 + 42.6D. \quad (26)$$

Figure 4(c) shows that the amount of backlash is similar to Fig. 4(a), i.e., the payload has little effect on the backlash. Indeed, the statistical value of the Student's test shows that the payload effect is negligible because the test on the first coefficient β_0' gives $t = -1.37 < 2.45$, so hypothesis H_0 is not rejected and the contribution of the coefficient β_0' is found insignificant at the threshold $\propto = 0.05$. As a result, the two curves are superposed, as seen in Fig. 6.

Similarly, results for the path parallel to the base y-axis with a payload of 2.23 kg and at a TCP speed of 10 mm/s show that after the lack-of-fit tests a second-order model is found sufficient to represent relationship between the backlash error and the robot configuration. Furthermore, the Student's test suggests that the relationship between the TCP speed and backlash is simply an offset (Fig. 7). The approximated model is

$$\hat{y}_i = -63.8 + 0.0241x_i - 0.00001x_i^2 + 52.44D. \quad (27)$$

The Student's test also shows that there is no relationship between payload and backlash (Fig. 8).

In order to show the usefulness of the used approach, the method is evaluated by comparing the residual between the experimental data for the no-loaded backlash and the experimental data for loaded backlash with the repeatability of the robot. A closer look at Figs. 6 and 8 shows that as the payload is increased, the backlash is constantly shifted negatively for the z-direction and positively for the y-direction. However, the data analyses show that the difference between the no-loaded experimental backlash and the loaded experimental backlash are between 2 μm and 10 μm for the y-axis and 5 μm and 9 μm for the z-axis, which are within the unidirectional repeatability. These results confirm the conclusion of the Student's test that there is no relationship between payload and backlash at 3σ repeatability.

Figures 9 and 10 show the relationship between the TCP speed and the backlash error at three selected TCP speeds. We can observe that the backlash errors in Fig. 9 are positive and increase as the TCP speed increases. However, Fig. 10 shows that the backlash errors for the path parallel to the y-axis are negative and decrease as the TCP speed increases. The positive sign of the backlash for the z-axis may have been caused by gravity on the end-effector of the robot moving along the vertical direction. Furthermore, the backlash error appears to have very different behavior, which is, however,

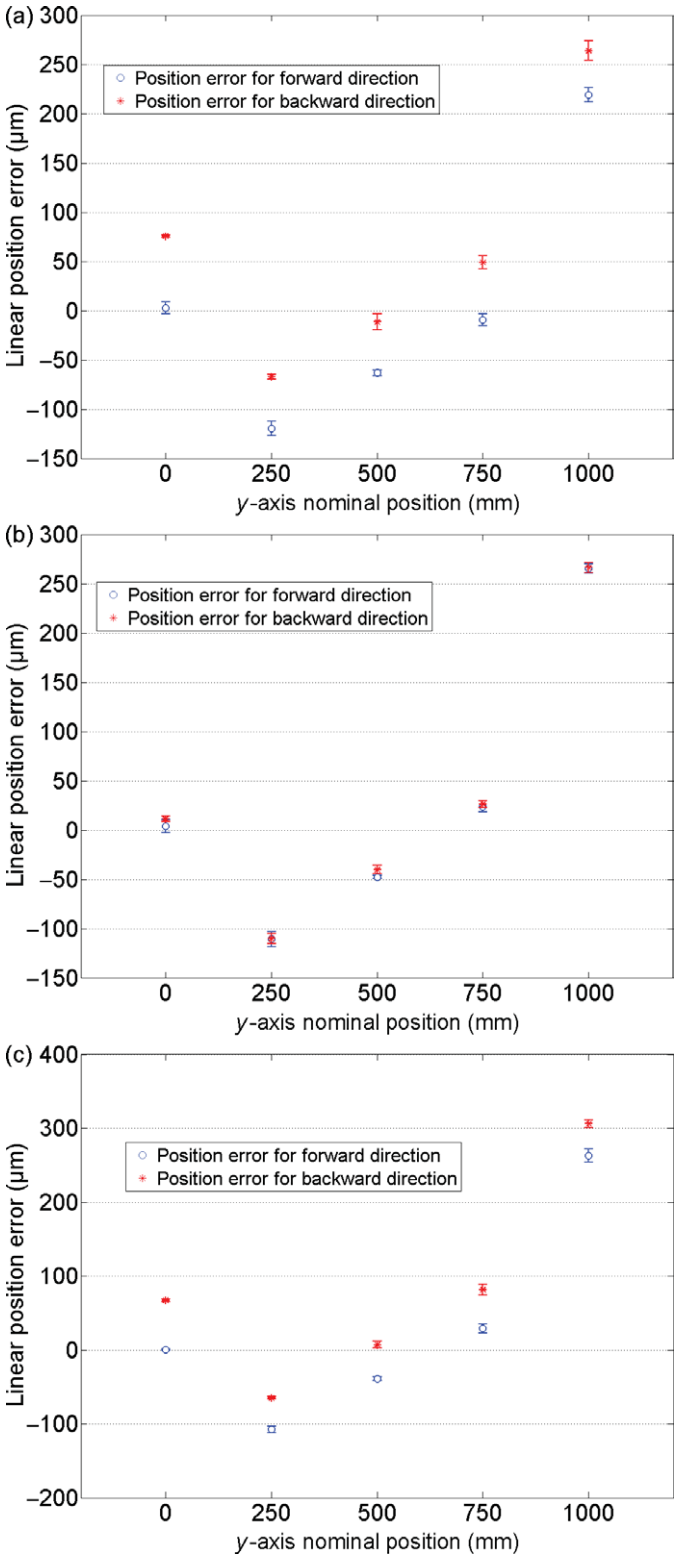

Fig. 4. (Colour online) Linear bidirectional position errors at five poses along the path parallel to the base y-axis. (a) Payload of 2.23 kg, TCP speed of 10 mm/s, $3\sigma_i^{\uparrow}$, $3\sigma_i^{\downarrow}$, and R_i are between 2 μm and 7 μm, 1 μm and 10 μm, and 62 μm and 80 μm, respectively; (b) payload of 2.23 kg, TCP speed of 6000 mm/s, $3\sigma_i^{\uparrow}$, $3\sigma_i^{\downarrow}$, and R_i are between 2 μm and 8 μm, 3 μm and 5 μm, and 11 μm and 17 μm, respectively; (c) payload of 6 kg, TCP speed of 10 mm/s, $3\sigma_i^{\uparrow}$, $3\sigma_i^{\downarrow}$, and R_i are between 1 μm and 9 μm, 1 μm and 7 μm, and 49 μm and 69 μm, respectively.

https://doi.org/10.1017/S0263574711001287 Published online by Cambridge University Press

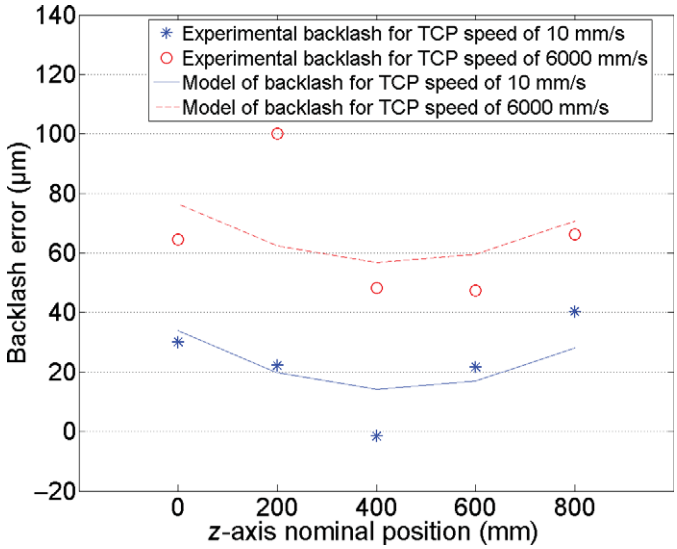

Fig. 5. (Colour online) Assessment of the effect of the TCP speed on the backlash at five equidistant poses along the path parallel to the base z-axis.

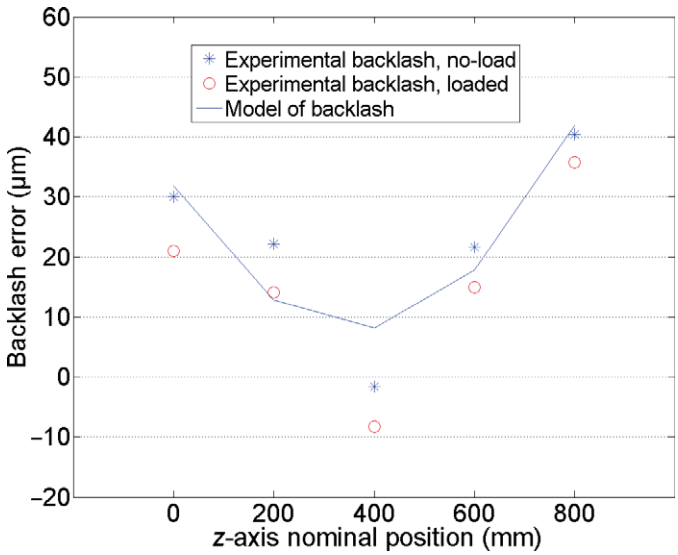

Fig. 6. (Colour online) Assessment of the effect of the payload on the backlash at five equidistant poses along the path parallel to the base z-axis.

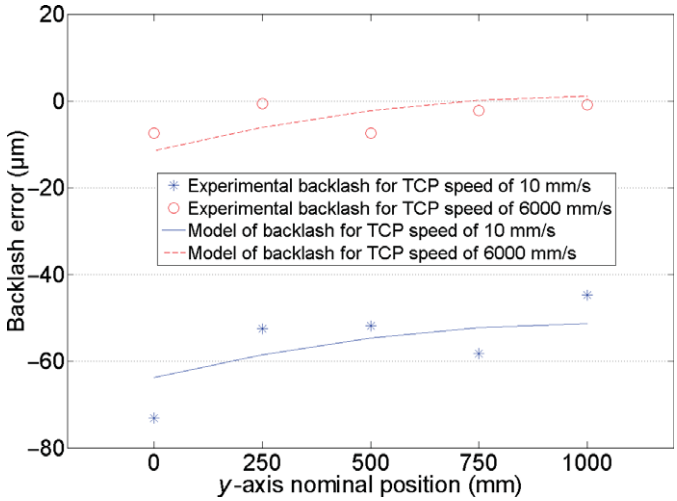

Fig. 7. (Colour online) Assessment of the effect of the TCP speed on the backlash along the path parallel to the y-axis.

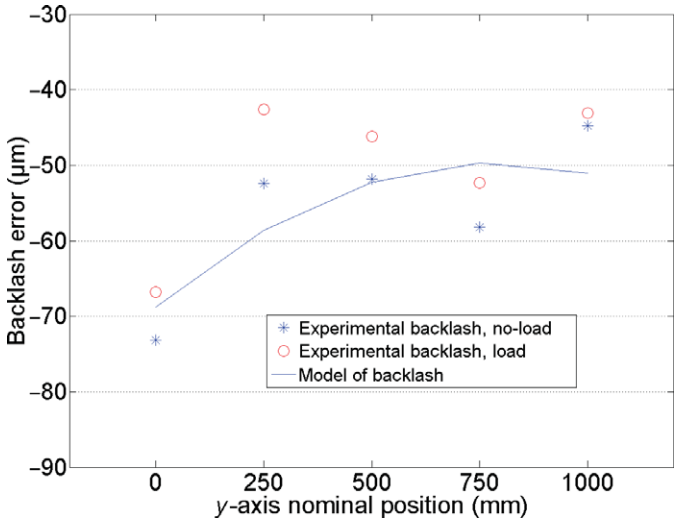

Fig. 8. (Colour online) Assessment of the effect of the payload on the backlash along the path parallel to the y-axis.

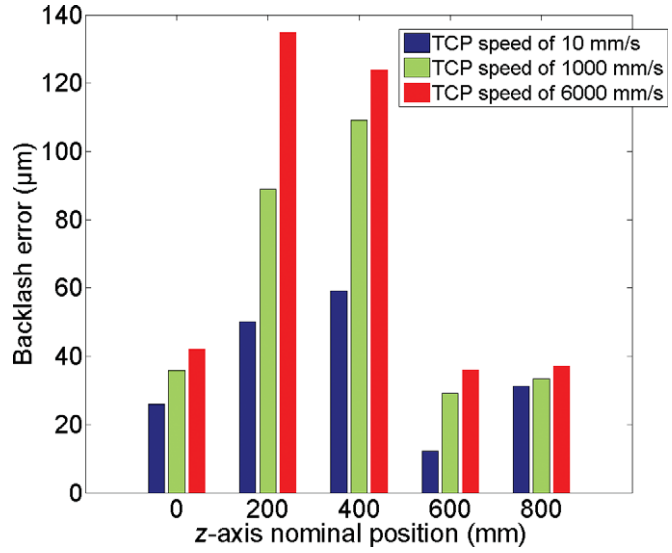

Fig. 9. (Colour online) Relationship between the TCP speed and backlash at five equidistant poses along the path parallel to the base z-axis.

not true. It can be inferred from this that the inertia effect of moving parts increases in proportion to their mass and acceleration. When the end-effector of the robot moves to the same nominal pose with different TCP speeds, the faster it moves the larger is the inertial effect, resulting in farther movement past the nominal stopping pose (case of positive position errors). This effect occurs both in the forward and backward directions, thus increasing the positive backlash, as can be seen in Fig. 9. In contrast, the negative backlash, as shown in Fig. 10, decreases as the TCP speed increases.

5. Conclusion

In this paper, an experimental approach based on statistical tests is presented to assess a relationship between robot configuration, TCP speed, and payload versus backlash error for an ABB IRB 1600 six-axis industrial serial robot. Polynomial model was used to represent the backlash error.

https://doi.org/10.1017/S0263574711001287 Published online by Cambridge University Press

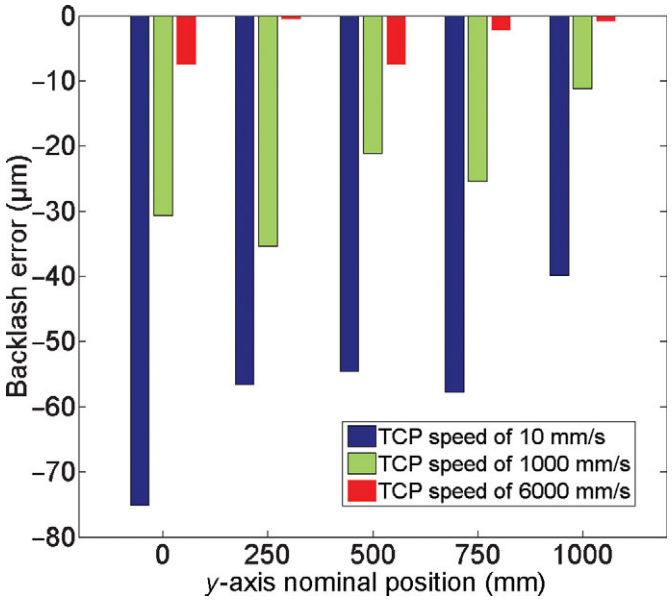

Fig. 10. (Colour online) Relationship between the TCP speed and backlash at five equidistant poses along the path parallel to the base *y*-axis.

The coefficients of polynomial functions are calculated by solving a linear system composed of the observation matrix and instrument readings. To choose the degree of polynomial and evaluate the contribution of the TCP speed and payload, two statistical tests, the lack-of-fit and the Student's tests, were successfully applied.

The results showed that the bidirectional repeatability is strongly affected by the backlash error, reaching in some cases 134 μm. The analysis also shows that the relationship between the backlash error and the robot configuration is well represented by a polynomial model of degree 2. Furthermore, the contribution of the TCP speed is significant and generally well modeled by a constant offset. Statistical tests also show that variation in payload has insignificant contribution and does not influence the backlash error.

Finally, an interesting behavior of the backlash was observed; that is, the positive backlash increases as the TCP speed increases and the negative backlash decreases as the TCP speed increases.

Acknowledgments

We would like to thank the Canada Foundation for Innovation (CFI) and the Canada Research Chair program for financial supporting of this work.

References

1. M. Summers, "Robot capability test and development of industrial robot positioning system for the aerospace industry," *Proceedings of the SAE 2005 AeroTech Congress & Exhibition*, Grapevine, TX, USA, Paper No. 2005-01-3336 (2005).
2. International Standardisation Organisation, "Manipulating industrial robots–performance criteria and related test methods," *ISO 9283* (ISO, Geneva, Switzerland, 1998).
3. S. Hayati, K. Tso and G. Roston, "Robot Geometry Calibration," **In**: *Proceedings of the 1988 IEEE International Conference on Robotics and Automation*, Pasadena, CA, USA (1988), vol. 942, pp. 947–951.
4. K. Young and C. G. Pickin, "Accuracy assessment of the modern industrial robot," *Ind. Robot: Int. J.* **27**(6), 427–436 (2000).
5. N. G. Dagalakis and D. R. Myers, "Adjustment of robot joint gear backlash using the robot joint test excitation technique," *Int. J. Robot. Res.* **4**(2), 65–79 (1985).
6. N. Sarkar, R. E. Ellis and T. N. Moore, "Backlash detection in geared mechanisms: Modeling, simulation, and experimentation," *Mech. Syst. Signal Process.* **11**(3), 391–408 (1997).
7. D. E. Whitney, C. A. Lozinski and J. M. Rourke., "Industrial robot forward calibration method and results," *J. Dyn. Syst. Meas. Control* **108**(1), 1–8 (1986).
8. M. F. M. Lima, J. A. T. Machado and M. Crisostomo, "Experimental backlash study in mechanical manipulators," *Robotica* **29**(2), 211–219 (2011).
9. A. Azenha and J. A. T. Machado, "Variable structure control of robots with nonlinear friction and backlash at the joints," **In**: *Proceedings of the IEEE International Conference on Robotics and Automation*, Minneapolis, MN, USA (1996) pp. 366–371.
10. C. Ma and Y. Hori, "The application of fractional order control to backlash vibration suppression," **In**: *Proceedings of American Control Conference*, Boston, MA, USA (2004) pp. 2901–2906.
11. Z. Q. Mei, R. Q. Yang, Ch. Liang and G. B. Li, "The study of backlash compensation and its application in the robot checking the filter," *Int. J. Adv. Manuf. Technol.* **25**, 396–401 (2005).
12. M. Ruderman, F. Hoffmann and T. Bertram, "Modeling and identification of elastic robot joints with hysteresis and backlash," *IEEE Trans. Ind. Electron.* **56**(10), 3840–3847 (2009).
13. International Standardisation Organisation, "Manipulating industrial robots–informative guide on test equipment and metrology methods of operation for robot performance evaluation in accordance with ISO 9283" *ISO TR 13309* (ISO, Geneva, Switzerland, 1995).
14. M. Slamani, A. Nubiola and I. A. Bonev, "Assessment of the positioning performance of an industrial robot," *Ind. Robot: Int. J.* 39 (1), (2012), http://www.emeraldinsight.com/journals.htm?articleid=1958519.
15. M. Slamani, J. R. R Mayer and G. M Cloutier, "Modeling and experimental validation of machine tool motion errors using degree optimized polynomial, including motion hysteresis," *Exp. Tech. J.* **35**(1), 37–44 (2011).
16. M. L. Berenson, D. M. Levine and M. Goldstein, *Intermediate Statistical Methods and Applications: A Computer Package Approach* (Prentice-Hall, Englewood Cliffs, NJ, 1983).
17. International Standardisation Organisation "Test Code for Machine Tools – Part 2: Determination of Accuracy and Repeatability of Positioning of Numerically Controlled Axes," 2nd ed. *ISO 230–2* (ISO, Geneva, Switzerland, 1997).

https://doi.org/10.1017/S0263574711001287 Published online by Cambridge University Press